Experimental and numerical comparison of currently available reaction mechanisms for laminar flame speed in 70/30 (%vol.) NH3/H2 flames

A Alnasif, Seif Zitouni, S Mashruk, Pierre Brequigny, M Kovaleva, Christine Mounaïm-Rousselle, A Valera-Medina

Experimental and Numerical Comparison of Currently Available Reaction Mechanisms for Laminar flame speed in 70/30 (%vol.) NH_3/H_2 Flames

ALNASIF A [1, 2,*], ZITOUNI S [3], MASHRUK S[1], BREQUIGNY P[3], KOVALEVA M[1], MOUNAIM-ROUSSELLE C[3], VALERA-MEDINA A[1]

[1] College of Physical Sciences and Engineering, Cardiff University, Wales, CF243AA, UK, alnasifah@cardiff.ac.uk
[2] Engineering Technical College of Al-Najaf, Al-Furat Al-Awsat Technical University, Najaf, 31001, Iraq.
[3] Université Orléans, INSA-CVL, EA 4229 – PRISME, F-45072, France.

ABSTRACT

To attain zero carbon emissions and mitigate carbon imprint on the environment, Ammonia is gaining traction as a promising alternative fuel to replace hydrocarbon fuels. However, the combustion characteristics of ammonia as fuel in a combustion system need to be investigated and examined. The aim of the current study is to analyse the laminar flame speed, a fundamental physio-chemical property of any combustible mixture, by means of experimental measurements and kinetic reaction mechanism analysis. Dealing with kinetic mechanisms can reveal the chemistry behind the reaction kinetics, which in turn can be used to analyse and improve the characteristics of ammonia as a fuel. The current study involved a series of experiments using the spherical expanding flame set-up to measure the laminar flame speed of 70/30 (%vol) NH_3/H_2 at atmospheric pressure and ambient temperature across a wide range of equivalence ratios (0.6-1.4). The study also included analysing 36 kinetic reaction mechanisms in order to appraise their performance with respect to laminar flame speed prediction for the measured NH_3/H_2 mixture. Absolute percentage error (APE) formula has been adopted for preliminary estimation based on the experimental measurements of the present study and numerical data. The study found that Duynslaegher et al., 2012 kinetic model shows good performance in the prediction of laminar flame speed across lean and stoichiometry conditions with a minimum value of APE in the range 0%-6%. The mechanism of Nakamura et al., 2017 demonstrates good estimation of laminar flame speed under rich conditions as well as that of Gotama et al., 2022. The sensitivity analysis of the laminar flame speed revealed the most important kinetic reactions in the promotion and retarding the laminar flame speed of 70/30 (%vol) NH_3/H_2 mixture. The kinetic reactions of $H+O_2=O+OH$, $NH_2+NH_2=N_2H_2+H_2$, and $OH+H_2=H+H_2O$ are the most important reaction with considerable effect in promoting the laminar flame speed at all conditions, while the reactions of $H+O_2(+M)=HO_2+M$, $NH_2+H=NH+H_2$, and $NH_2+O=HNO+H$ play an important role in the retarding of laminar flame speed from lean to rich conditions. The effect of the aforementioned reactions varies with respect to the equivalence ratio, mainly due to changes in adiabatic flame temperature.

***Keywords**: Ammonia, Binary flames, Kinetic modelling, Laminar flame speed, Reaction mechanism.*

Introduction

Over the last century, the energy needs of our society have been largely supported by the abundance of cheap hydrocarbon-based fuels, accounting for nearly three-quarters of our global primary energy consumption [1]. Declining indigenous resources coupled with the well-established environmental and ecological adversities resulting from hydrocarbon combustion have helped strive to focus on the study of alternative fuel sources [2]. In this regard, ammonia (NH_3) has received a lot of attention lately [3–5], as an efficient zero-carbon energy carrier. NH_3 offers higher gravimetric H_2 content than for example methanol, gasoline, and ethanol [4–6] and can be synthesized from fossil fuels, or renewable energy sources coupled with an already mature infrastructure and storage system[4,7]. As such, NH_3 has become a promising alternative fuel, with its utilization demonstrated in high-pressure energy systems such as industrial gas turbines and gas engines [3–5,8,9]. However, several combustions feature of these flames require further understanding.

The Laminar flame speed is a fundamental physiochemical property of a premixed combustible mixture, resulting from the shared influence of mass and thermal diffusion of the reactants and mixture exothermicity [10]. The laminar flame speed reflects both the combustion process and a characterisation of a given fuel blend, rendering the laminar flame speed a key parameter in helping describe premixed operational instabilities (for

example, flash-back, blow-off, and extinction). The laminar flame speed is defined as the velocity a steady one-dimensional adiabatic flame front propagates normal to itself in the doubly infinite domain. This definition renders the laminar flame speed particularly suitable for calculations in one-dimensional simulation which rely on thermodynamic and transport data, and thus by extension convenient in appraising and validating chemical kinetic mechanisms and models [10,11].

The laminar flame speed of NH_3 known as very low, peaking at slightly rich conditions (equivalence ratio (φ) of ~ 1.05-1.10), at a value of around 7cm/s, [3]. Such slow-burning velocities are often associated with low burning efficiencies in engines, potentially yielding poor flame stabilization resulting in local or global extinction. As such, to improve NH_3's combustion characteristics, blending with methane (CH_4) [12,13], or H_2 [14], as well as oxy-combustion [15,16] has been proposed. In this study, a NH_3-H_2 fuel mixture composition of 70-30 (%vol.) has been chosen due to its stable performance in fuelling gas turbine combustors [4,17]. The addition of H_2 to NH_3 results in an increase in burning rate[18], enhanced the reactivity of the mixture [19], and widened flammability limits [8].However, the NH_3-H_2 fuel blend has several drawbacks, notably due to higher flame temperatures and abundance of radicals, such as OH, O, and H, potentially causing an increase in NOx formation [20,21], a detrimental greenhouse gas pollutant.

Recently, significant efforts have been undertaken to establish kinetic models that are able to predict the combustion characteristics of NH_3-H_2 flames, including the commendable efforts to understand ammonia reaction chemistry from various groups worldwide [22–25]. The optimization process for NH_3-H_2 chemistry entails a specific understanding of the chemistry of each component of fuel and their interactions. Similarly, a chemical kinetic model has also been established by [26] for ammonia oxidation based on experimental measurements taken inside a shock tube. The resulting mechanism has also been compared with 9 other kinetic mechanisms from the literature [26]. Glarborg [22] developed a comprehensive kinetic model including an overview of the most recent data in the kinetic modelling of ammonia combustion. The oxidation kinetic mechanism published by [25] for pure ammonia and ammonia-hydrogen flames has also received considerable attention, been validated for a number of 0D and 1D energy systems. Li et al. [27] led also to the development of two reduced models for NH_3-H_2 and NH_3-CH_4-H_2 fuel mixtures respectively. Similarly, many other research groups keep attempting to develop a mechanism that fully loosens the complexities of using ammonia blends with high accuracy for chemical and numerical studies.

As mentioned above, several numerical and experimental studies have been carried out to understand the combustion characteristics of NH_3-H_2 blends and their applicability in combustion-based systems. The present work deals with this problem by analysing the laminar flame speed of a highly stable 70-30 (%vol.) NH_3-H_2 fuel blend measured experimentally using a constant-volume spherical vessel, and numerically by modelling laminar flame speed and comparing 36 currently peer-reviewed chemical kinetic mechanisms. This sheds light on the performance of these mechanisms and the key kinetic reactions that promote the laminar flame speed. The results denote the most accurate mechanisms for various combustion conditions, whilst directing efforts of future works to improve these models for further utilization.

Methodology

Experimental work

Laminar flame speed measurements were performed using a constant-volume spherical vessel, Fig.1. Details of the rig and post-processing technique can be found in[28], updated for NH_3 specifications in [9] and thus only a brief summary is presented here. The spherical vessel has a nominal internal volume of 4.2 L (ID 200mm), with four orthogonal 70 mm quartz viewing windows with PID temperature control. High-speed Schlieren imaging of flame propagation was achieved using a CMOS high-speed camera (PHANTOM V1210) set to a suitable fast frame capture rate and facilitating a spatial resolution of ~0.1 mm per pixel. Flame propagation velocities were calculated by edge-detection algorithms written into a bespoke MATLAB script. Reactants were introduced into the chamber using batched thermal mass flow controllers (Brooks 5850S (±1%)). Mass fractions were calculated as a function of initial pressure (P), fuel-air equivalence ratio (φ), and temperature (T), with mixture concentrations confirmed by partial pressure. Internal fans were used to pre-mix the reactants, and capacitor-discharge ignition was achieved via fine electrodes mounted to 45° to the measurement plane.

Experiments were triggered by a simultaneous TTL signal to the ignition system and data acquisition systems after quiescence had been attained. High-purity fuel components of H_2 (>99.95%) and NH_3 (99.95%) and dried compressed air were used to perform the experiments. Measurements were performed at initial conditions of 298 K (± 3K) and 0.1MPa (± $1x10^{-3}$Mpa). To investigate the influence of H_2 on NH_3 flame propagation, spherically expanding flame experiments were conducted for a set molar ratio of H_2 (30%, vol), evaluated across a wide range of equivalence ratio (φ), to provide a comparison of the change in flame speed from lean to rich conditions. Schlieren measurements were undertaken to evaluate the laminar flame speed relative to the burned side and were experimentally determined by employing the same procedure as in previous studies [9,29]. Figure 2 illustrates an example of images underlining the quality of images taken using the Schlieren optical set-up.

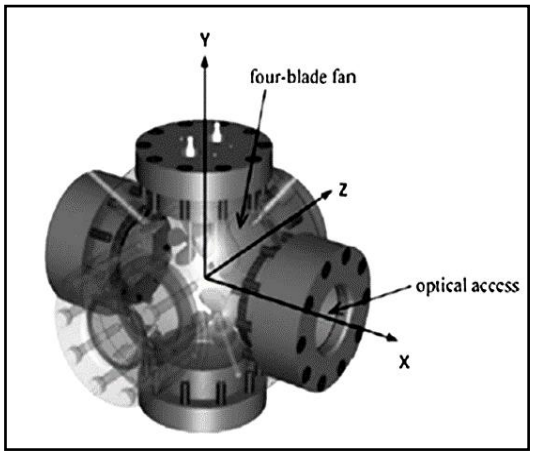

Fig. 1. Schematic of Constant Volume Combustion Vessel

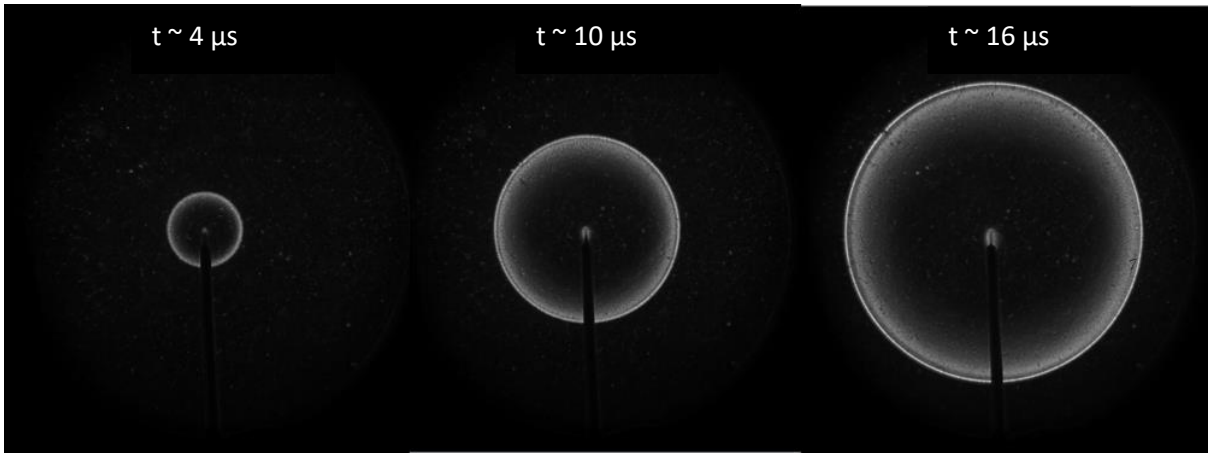

Fig.2. Temporal evolution of a spherically expanding 70-30 (%vol.) NH_3-H_2 flame using Schlieren (φ=1.0, T_u=298K, P_u = 0.1MPa)

For an outwardly propagating flame, the stretched flame speed (S_n) is expressed as the temporal derivative of the Schlieren flame radius (r_{sch}) as per Equation 1

$$S_n = \frac{dr_{sch}}{dt} \qquad \text{(Equation 1)}$$

A quasi-steady non-linear association between S_n and stretch, as proposed by [30] was utilized to obtain an extrapolated unstretched flame speed (S_b), that allows for arbitrary Lewis Number and accounts for deviations in adiabatic and planar assumptions, prominent in flames which are heavily influenced by stretch such as lean H_2-based flames. To obtain an extrapolated unstretched flame speed, a quasi-steady non-linear association between S_n and α is employed (as in Equation 2), re-arranged with the error used for least square regression:

$$\left(\frac{S_n}{S_b}\right)^2 . ln\left(\frac{S_n}{S_b}\right)^2 = -\frac{2*L_b*\alpha}{S_b} \qquad \text{(Equation 2)}$$

Irrespective of the extrapolation methodology employed, to obtain representative values of laminar flame speed, the burned gas expansion must be factored as $U_L = S_b \cdot (\rho_b/\rho_u)$ with ρ_b and ρ_u, burnt and unburnt gases densities calculated using CHEMKIN-Pro.

Substantial efforts are being made to improve the accuracy of reaction mechanisms, which depend on accurate laminar flame speed measurements [31]. Uncertain quantification for the present measurements relies upon the methods outlined by [32], employing a combination of the experimental facility specification and accuracy of the processing techniques chosen. It should be noted that the uncertainty is quantified for the unstretched

flame speed (S_b), (and not as opposed to LBV itself), since this is the parameter measured. The total uncertainty estimate is given by Equation 3, where (B_{Sb}) represents the total bias uncertainty, (tM-1,95) the student's t value at 95% confidence interval and M-1 degrees of freedom, (σ_{Sb}) is the standard deviation of the repeated experiments, and (M) the number of experimental repeats at each condition [9,33].

$$U_{sb} = \sqrt{B_{sb}^2 + \left(\frac{t_M - 1.95\sigma_{su}}{\sqrt{M}}\right)^2} \qquad \text{(Equation 3)}$$

The total bias uncertainty, given by Equation 4, relates changes in S_b with respect to an independent influential variable vi (i.e., temperature, ambient pressure, φ) and the fixed error linked to that variable -yi-.

$$B_{sb} = \sqrt{\sum_{i=1}^{n}\left(\frac{\partial S_b(v_i)}{\partial v_i} y_i\right)^2} \qquad \text{(Equation 4)}$$

In order to employ Eqn. 4, the relationships between S_b and each independent variable must be established. The potential changes in S_b from several parameters are calculated as a function of φ; such as temperature (±3 K), and pressure (±1 x 10^{-3} MPa), with the relationship proposed by [31] employed to evaluate the uncertainty in global φ. Data modelling employing CHEMKIN-PRO was utilised to estimate these profiles. Uncertainty resulting from the optical system was evaluated from the summated fractional error of both the spatial resolution of the system (±0.05/25mm) and camera (± 1.5/3000fps). Additionally, Wu et al.,[34] quantified the uncertainty in extrapolation, with corresponding $Ma_{lin}Ka_{mid}$ values for data presented in this work falling within the recommended range of -0.05 – 0.15. Accordingly, error bars on all subsequent plots illustrating laminar flame speed measurements are derived from Eqn. 3 & 4, with the error for U_{Su} scaled with respect to the density ratio. A minimum of 5 repeats were conducted per each experimental condition.

Kinetic modelling

The analysis of 36 kinetic reaction mechanisms has been performed employing the ANSYS CHEMKIN-PRO software. A premixed laminar flame-speed calculation model was applied for all reaction mechanisms. The numerical calculations for all model tests were done in a one-dimensional computational domain of length 10 cm, with a maximum grid size of 5000. The adaptive grid control based on solution gradient and curvature was set to 0.02. The grid dependency has been taken into account and the accuracy for all cases was tested and adjusted to give precise results. Table 1 illustrates each mechanism's details regarding the number of reactions and species adopted.

Table 1: Chemical kinetic mechanisms used in the present work

No.	Kinetic mechanism	No. of Reactions	No. of species	Ref.	No.	Kinetic mechanism	No. of Reactions	No. of species	Ref.
1	(Bertolino et al., 2021)	264	38	[35]	19	(San Diego Mechanism, 2018)	41	20	[36]
2	(Mei et al., 2021a)	264	38	[37]	20	(Klippenstein et al., 2018)	211	33	[23]
3	(Han et al., 2021)	298	36	[38]	21	(Nakamura et al., 2017)	232	33	[39]
4	(Mei et al., 2021b)	257	40	[21]	22	(Zhang et al., 2017)	251	44	[40]
5	(Gotama et al., 2022)	119	26	[41]	23	(Lamoureux et al., 2016)	934	123	[42]
6	(Shrestha et al., 2021)	1099	125	[24]	24	(Xiao et al., 2016)	276	55	[43]
7	(Wang et al., 2021)	444	91	[44]	25	(Song et al., 2016)	204	32	[45]
8	(Zhang et al., 2021)	263	38	[46]	26	(Nozari and Karabeyoɬlu, 2015)	91	21	[47]
9	(Arunthanayothin et al., 2021)	2444	157	[48]	27	(Mathieu and Petersen, 2015)	278	54	[26]
10	(Stagni et al., 2020)	203	31	[49]	28	(Duynslaegher et al., 2012)	80	19	[50]
11	(Han et al., 2019b)	177	35	[51]	29	(Klippenstein et al., 2011)	202	31	[52]
12	(De Persis et al., 2020)	647	103	[53]	30	(Zhang et al., 2011)	701	88	[54]
13	(Mei et al., 2019)	265	38	[55]	31	(Lamoureux et al., 2010)	883	119	[56]
14	(Li et al., 2019)	957	128	[27]	32	(Konnov, 2009)	1207	127	[57]
15	(Okafor et al., 2019)	356	59	[58]	33	(Mendiara and Glarborg, 2009)	779	79	[59]
16	(Glarborg et al., 2018)	231	39	[22]	34	(Tian et al., 2009)	703	84	[60]
17	(Shrestha et al., 2018)	1081	124	[25]	35	(Dagaut et al., 2008)	250	41	[61]
18	(Otomo et al., 2018)	213	32	[62]	36	(GRI-Mech 3.0., 2000)	325	53	[63]

Results and discussion

This section addresses the laminar flame speed modelled by 36 kinetic reaction mechanisms, compared to the experimental results conducted in the present study and measurements reported by previous studies [9,14,21].

To determine the best performing kinetic mechanism for predicting the laminar flame speed of 70/30 (%vol.) NH_3/H_2 flames at atmospheric conditions, the absolute percentage error (APE) formula has been adopted as preliminary estimation criterion [64], to calculate the error percentage between the predicted numerical data and experimental results for various equivalence ratios (φ=0.6-1.4).

Lean and stoichiometry condition flames

Figure 3 shows the absolute percentage error estimated for 36 kinetic reaction mechanism using the experimental measurements curried out in the present study. For an equivalence ratio of 0.6, the Duynslaegher's model [50] provides good agreement with experimental results with an error equal to 2% followed by Song [45], Klippenstein[52], and Nakamura's [39], with around 4% of relative error for each mechanism, respectively. At φ = 0.8, Lamoureux et al.,[56] mechanism demonstrated to be the best mechanism in the estimation of laminar flame speed with a minor error of just 1%. On the other side, the relative error for Duynslaegher was recorded at around 6%, as can be seen in Fig. 3. When the equivalence ratio is at stoichiometry, Duynslaegher is the best performing mechanism with 0% relative error. Therefore, the Duynslaegher mechanism shows an excellent prediction for the laminar flame speed measurement not only in the stoichiometric conditions but also under lean conditions (0.6-1.0)

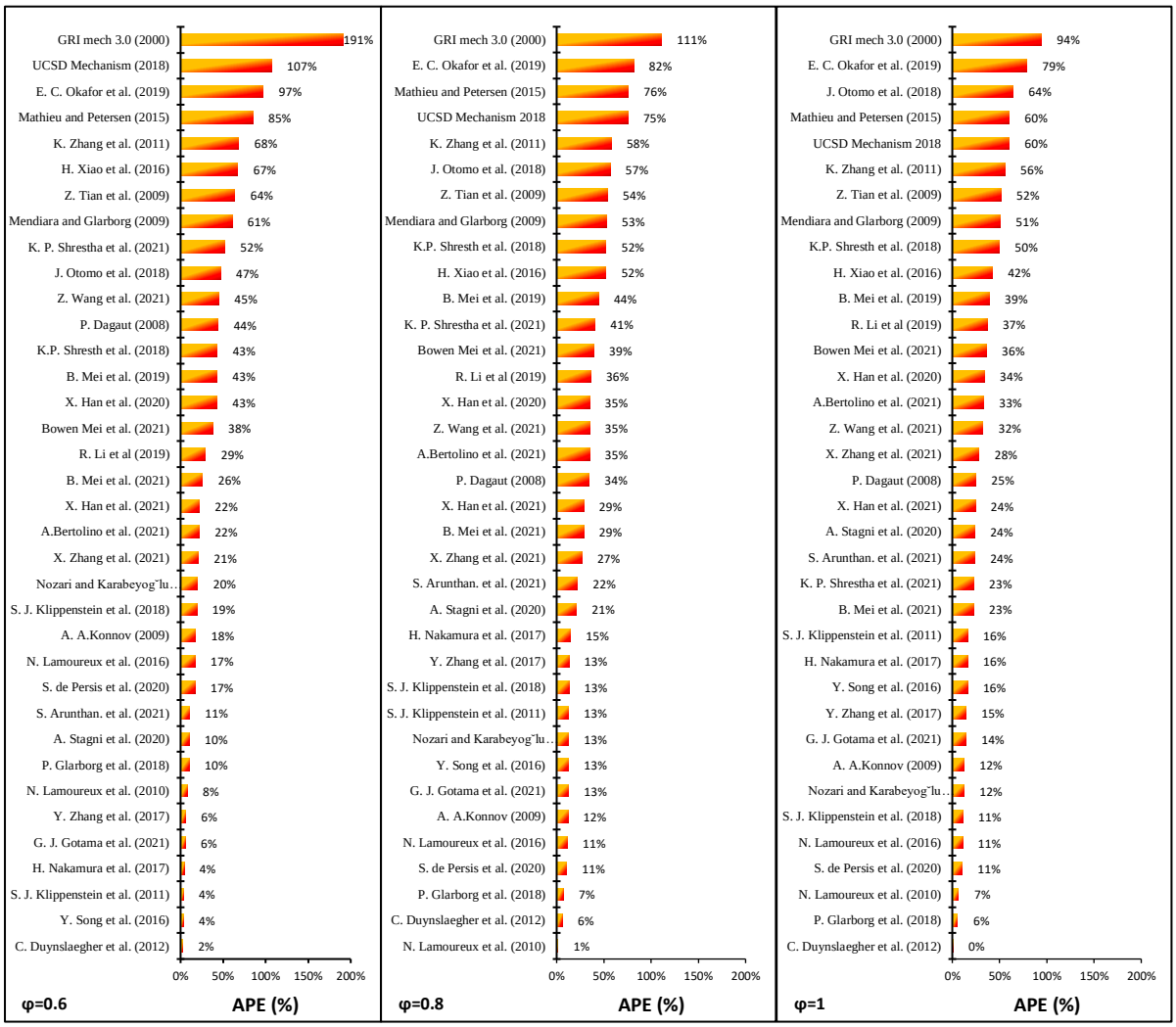

Fig. 3. The relative error for 36 kinetic reaction mechanism for an equivalence ratio in the range of 0.6-1.0.

Figure 4 illustrates the predicted and measured laminar flame speed for 70/30 (%vol) NH_3/H_2 as a function of equivalence ratio (0.6-1.4). Good agreement is observed between the present experimental results and those of Lee et al. (**Add reference**) across the entire equivalence ratio range. Good agreement is also visible between present results and those of L'Huillier et al. [9], particularly at leanest and richest conditions. Some deviation is observable, particularly at φ = 0.9 and 1.0, with presented results significantly higher than those reported by L'huillier et al. [9]. It is also noted that data presented in this study and those of Lee et al. [Add ref] exhibit a classic bell shape curve, with greatest laminar flame speed measured at φ = 1.0, whilst measurements by L'huillier et al. [9] peak at an φ = 1.1, as well as exhibiting a spurious flame speed at φ = 1.3, not measured by other researchers nor predicted by the selected kinetic reaction mechanisms. Glarborg [22] , Lamoureux [56], and Duynslaegher [50] mechanisms display good agreement with the experimental measurements in the lean conditions. In spite of there being an underestimation of the laminar flame speed at φ = 0.8, the mechanism of Duynslaegher has a minimum level of discrepancy against the experimental data. The Lamoureux mechanism has good performance at lean conditions and gives only a slight underestimation of laminar flame speed at an φ = 0.6, with the error increasing at stoichiometry to give an overestimate of around 7% compared to experimental measurements, see Fig.3. The Glarborg kinetic model has a consistent trend line along with the experimental results with an overestimation value for the laminar flame speed between 6% to 10% and for all lean conditions and stoichiometry. Finally, the Gotama model shows peak divergence at stoichiometry, but performing fairly well at rich and very lean equivalence ratio conditions.

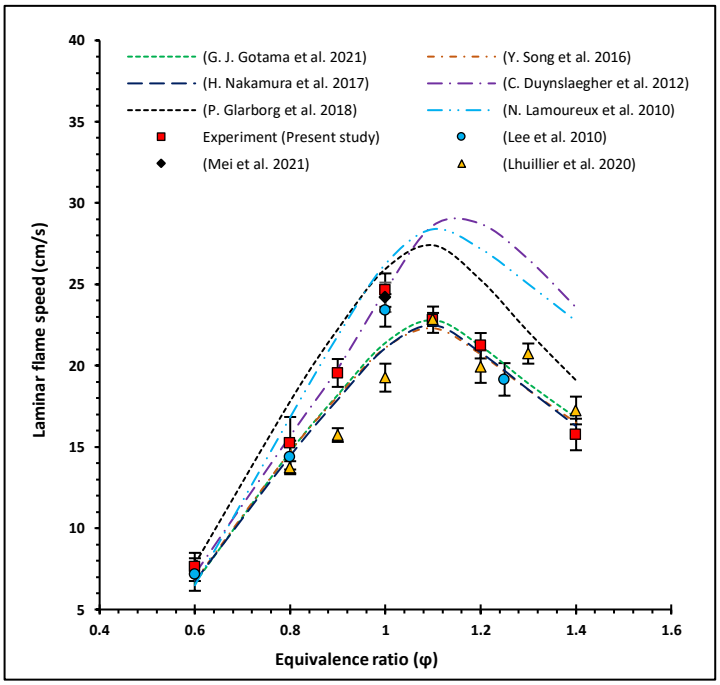

Fig. 4: The laminar flame speed for 70/30 (%vol.) NH_3/H_2 flames predicted by six kinetic reaction mechanisms with low level of discrepancy for the full range of equivalence ratios (0.6-1.4), The dashed lines refer to the numerical data, while the symbols stand for the experimental measurements of the present study and reported measurements from the literature.

To analyse the flame speed sensitivity of 70/30 vol% NH_3/H_2 blended fuel, three kinetic reaction mechanisms have been selected (Gotama [41], Duynslaegher [50], and Glarborg [22]) based on their performance from lean to stoichiometric equivalence ratios. These mechanisms were chosen because the mechanism of Glarborg slightly overestimates the Laminar flame speed, and the Gotama mechanism slightly underestimates the Laminar flame speed, while the kinetic mechanism of Duynslaegher is in between both, with the lowest error of all.

Figure 5 shows the sensitivity coefficient of the mentioned selected mechanisms and demonstrates the most important reactions that promote/ retard the laminar flame speed. As can be seen from the figure, all the selected mechanisms show that the reactions $H+O_2=O+OH$, $OH+H_2=H+H_2O$, and $NH_2+NO=NNH+OH$ play a dominant part in boosting the laminar flame speed. While the reaction of negative sensitivity coefficient $H+O_2(+M) = HO_2(+M)$ has the most influence on retarding the laminar flame speed among other reactions with the same effect. Since the mechanism of Duynslaegher has a better prediction of the experimental data of laminar flame speed and with a minimum level of error values between 0% to 6% in the full range of the lean condition and stoichiometry, The reaction $H+O_2=O+OH$ recorded low level of sensitivity in comparison with the sensitivity coefficient of the same reaction provided by Glarbourg and Gotama kinetic models. Along with that, the sensitivity of this reaction increases gradually when the equivalence ratio increases from 0.6 to 1, whilst both the Glarborg and Gotama kinetic models show no change in the sensitivity values of the same reaction. In addition to that, the mechanism of Duynslaegher demonstrate good response to the kinetic reaction $H+O_2(+M) = HO_2(+M)$ in the retarding of the flame speed at φ=0.6, but the effect of the mentioned reaction has

no trace at 0.8 and 1 of φ. While both the Glarborg and Gotama kinetic models show the influence of the reaction $H+O_2(+M) = HO_2(+M)$ clearly along the lean range and stoichiometry (0.6-1 of φ).

The differentiation of the sensitivity coefficients among the selected mechanisms can be justified to the variation of Arrhenius parameters that control the reaction rate of each kinetic reaction. Where the selected mechanisms demonstrate different values of Arrhenius parameters in their chemistry data base, Table 2. As shown in Table 2, the kinetic reaction '$OH+H_2=H+H_2O$' estimated by Gotama has large temperature dependence because of its large value of activation energy, while the same reaction that has been listed in both Duynslaegher and Glarborg mechanism database show low-temperature dependency due to low activation energy. So, the fact that most kinetic reactions are temperature dependent might be the reason behind the discrepancy matter in the prediction of laminar flame speed from one mechanism to another. Also, the difference in which kinetic reactions are included substantially affects the performance of the kinetic mechanism.

In terms of chemistry, all three mechanisms show different chemistry in terms of the most important reactions that affect the laminar flame speed of 70/30 vol% NH_3/H_2 blended fuel. At 0.6 of φ, the Duynslaegher kinetic model illustrates the positive effect of the reaction $N_2H_2+M=NNH+H+M$ on the promotion of the laminar flame speed, as well as the negative effect of the reactions $NH_2+H=NH+H_2$, and $NO+O=NO_2$ which cannot be seen in both Glarborg and Gotama mechanisms, Fig.5. The influence of the mentioned reactions extended to include other conditions of φ (0.8 and 1). Although Glarbourg and Gotama kinetic models sharing nearly the same chemistry, where both kinetic models show the effect of the reaction $NH_2+NH=N_2H_2+H$ in promoting the laminar flame speed and the retarding effect of the recation $NH_2+NO=N_2+H_2O$. Gotama kinetic model also present the kinetic reactions $NH_2+NH=N2H_3$, $NH_2+OH=NH+H_2O$, and NH2+NH2=N2H3+H that cannot be found in Glarbourg chemistry data base, instead, the Mechanism of Glarbourg include the kinetic reactions $HNO+H=NO+H_2$, $NH+NO=N_2O+H$ at 0.6 and 0.8 of φ, and $NH+H_2=NH_2+H$, $NH_2+H(+M)=NH_3(+M)$, and NH+O=NO+H at stoichiometry, Fig.5.

Table 2: Key reactions and their rate constants generated from Gotama, Duynslaegher, and Glarborg mechanisms.

NO.	Reaction	Gotama et al. (2022)			Duynslaegher et al. (2012)			Glarborg et al. (2018)		
		A	n	E	A	n	E	A	n	E
1	$H+O_2=O+OH$	5.0712E+015	-0.49	16126.7	9.75E+13	0.0	14900	1.0E14	0	15286
2	$H+O_2(+M) =HO_2(+M)$	4.65E+12	0.4	0	1.48E+12	0.6	0	4.70E+12	0.40	0
3	$OH+H_2=H+H_2O$	4.38E+13	0	6991	1.00E+08	1.6	3300	2.2E+08	1.5	3430
4	$NH_2+NO=NNH+OH$	1.43E+07	1.4	-1777	2.29E+10	0.425	-814	4.3E+10	0.29	- 866

To see the effect of Arrhenius parameters on the laminar flame speed, the Rate of Reaction for the most effective reactions on the laminar flame speed has been plotted at 0.6 of the equivalence ratios. As shown in Fig. 6, the reaction rate of $H+O_2=O+OH$, $H+O_2(+M)=HO_2(+M)$, and $NH_2+NO=NNH+OH$ predicted by the Glarborg mechanism were larger than those estimated by both Gotama and Duynslaegher mechanisms and this effect also reflected on the temperature plots for the mentioned mechanisms, where temperature profile estimated by Glarborg model reaction recorded higher value than the other two reaction mechanisms at the position where maximum heat release rate takes place. In addition to that, the peak values of the reaction rate of the mentioned reactions that are estimated by Gotama's mechanism nearly swept to the right compared with peak values for the same reactions calculated by Glarborg and Duynslaegher which are aligned. Further, the reaction rate profiles of '$H+O_2(+M)=HO_2(+M)$' for all three mechanisms give the same trend, which is in spite of the peak values of this reaction taking place in the reaction zone, this kinetic reaction had the reaction continuous and in progress in the post flame region. Along with that, the reaction rate of the mentioned reaction predicted by the Duynslaegher mechanism rapidly decreased and reached almost zero around 5.13 cm in comparison to the same kinetic reaction calculated by Gotama and Glarbourg kinetic models that show a higher reaction rate in the same location and decreased gradually to reach nearly zero above 5.3 cm.

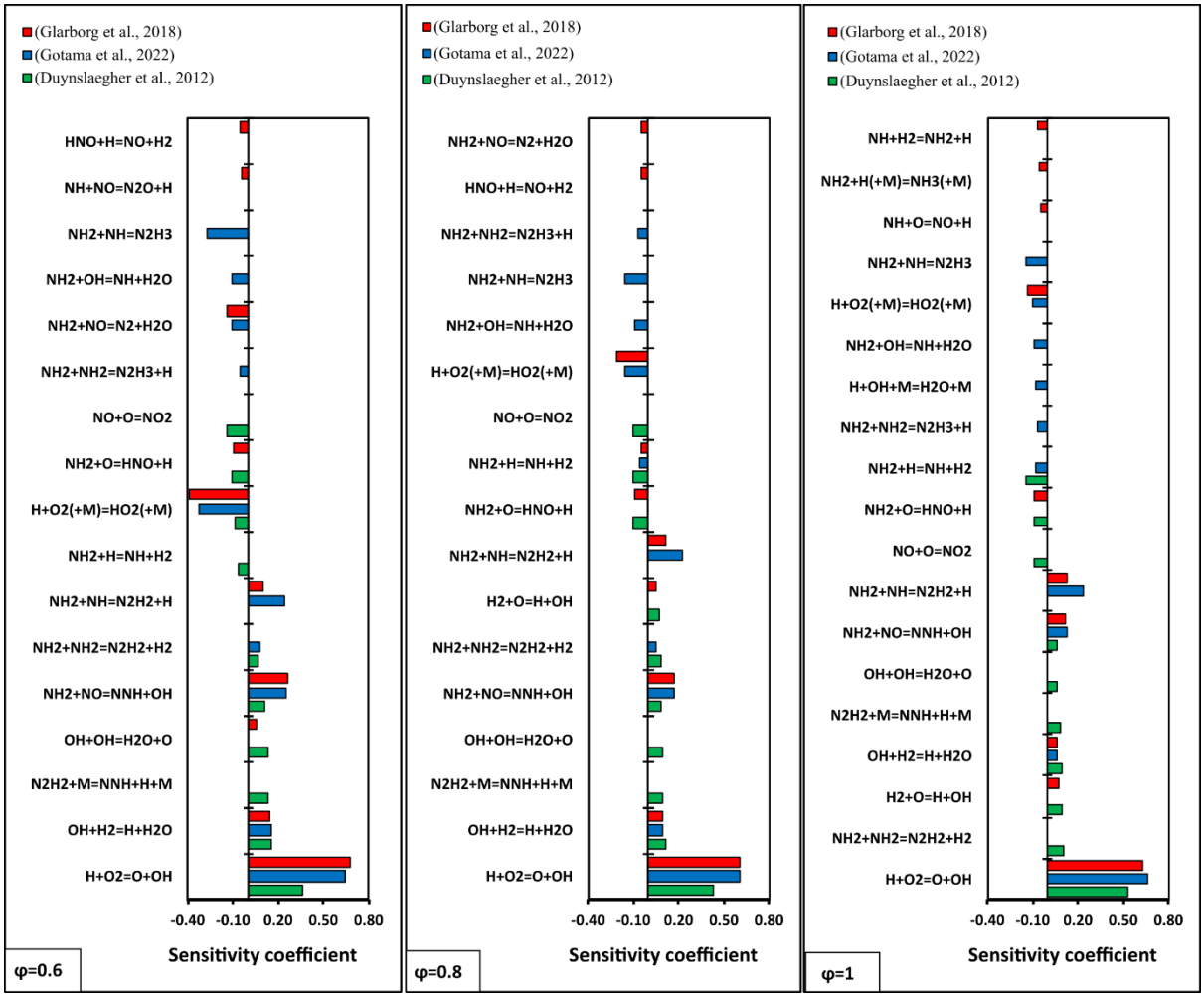

Fig. 5. Sensitivity analysis for laminar flame speed of 70/30 (%vol.) NH_3/H_2 under atmospheric conditions and for three kinetic mechanisms (Gotama et al. 2022, Duynslaegher et al. 2012, and Glarborg et al. 2018) that give a minimum discrepancy value at lean and stoichiometry conditions (0.6-1.0).

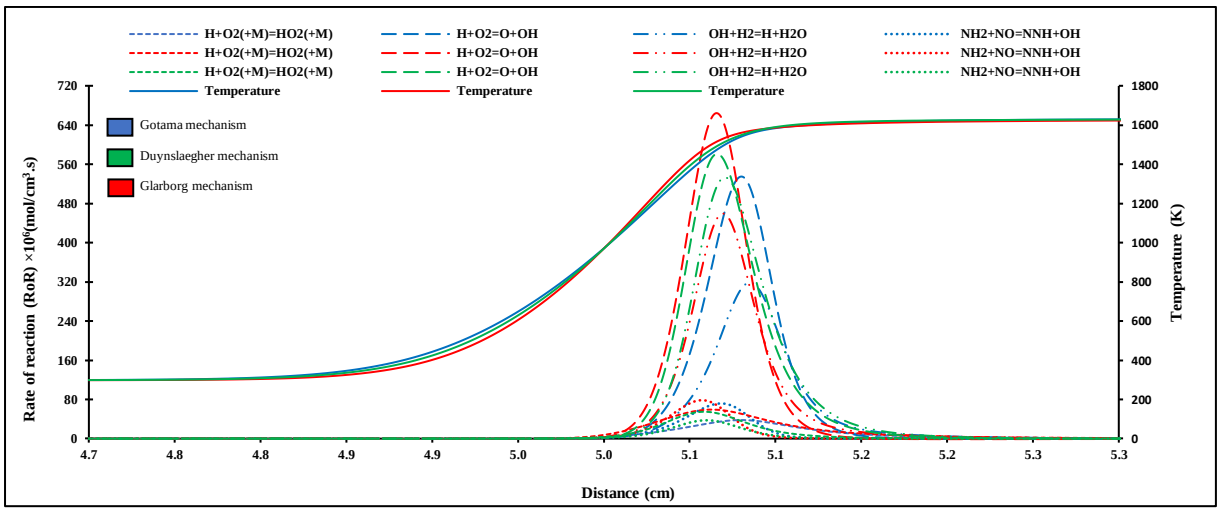

Fig. 6. The rate of reaction (RoR) profiles of the key reactions and temperature profiles for 70/30 (%vol.) NH_3/H_2 flames at φ= 0.6; sold lines refer to the temperature, while dashed lines refer to the rate of reaction.

Rich condition flames

Figure 7 refers to the Absolute Percentage Error (APE) estimated for laminar flame speed in the rich equivalence ratio conditions (1.1, 1.2 and 1.4). As can be seen Nakamura mechanism [39]gives a good estimate of flame speed with error values in the range 2%-8% along the rich conditions (1.1-1.4). Song mechanism [45]has similar performance, with some overestimate at 1.4 of φ. While Gotama's kinetic model [41] provides an excellent estimate at φ =1.1 and 1.2, this percentage is increased with increasing equivalence ratio to reach 8% at 1.4. Although Duynslaegher kinetic mechanism demonstrates a good estimation in the lean and stoichiometry conditions, its performance deteriorates at rich conditions with errors in the range 21% - 34%, as it is highlighted in Figs.4 and 7.

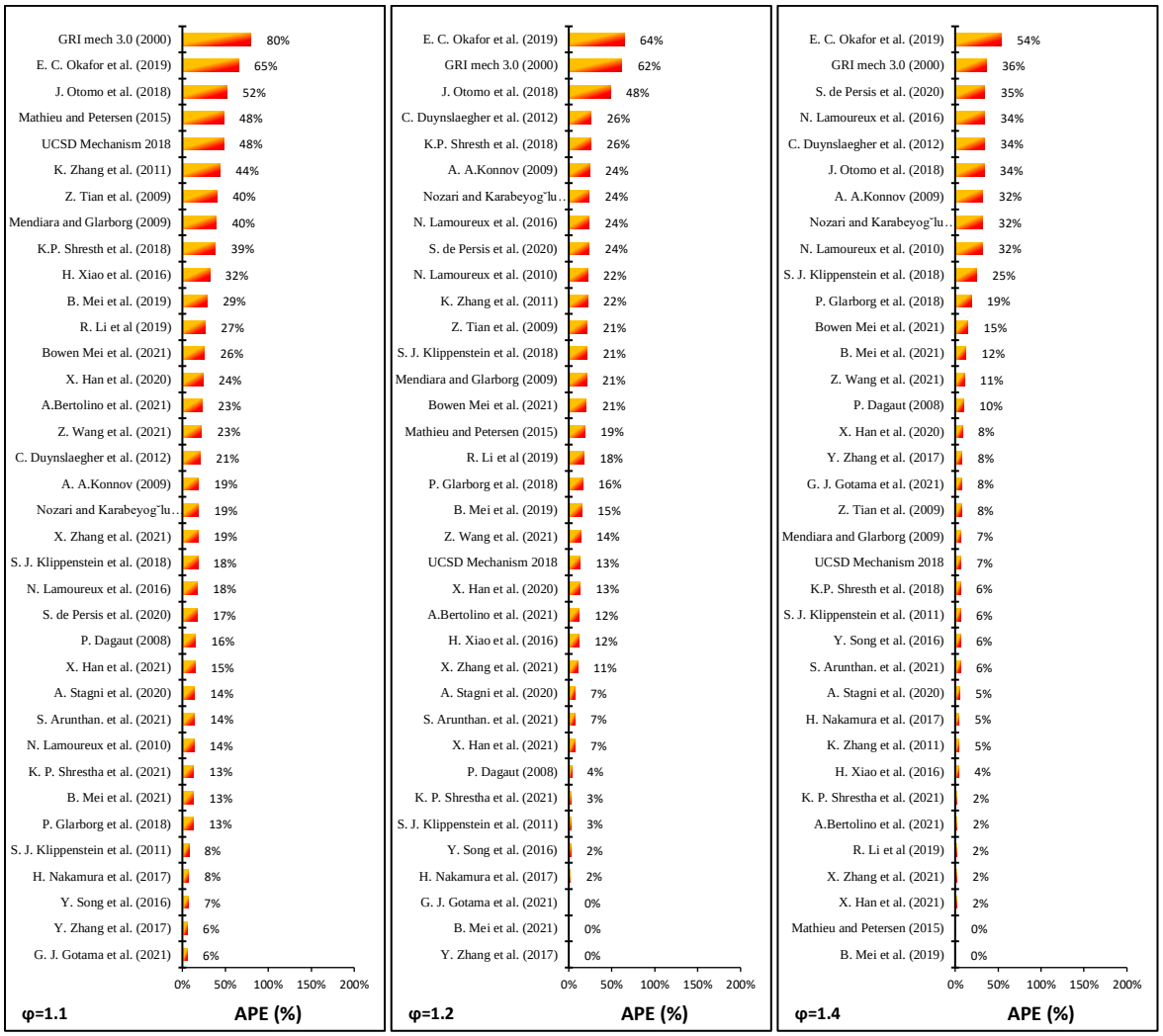

Figure 7: The Absolute Percentage Errors (APE) for the laminar flame speed predicted by 36 kinetic reaction mechanisms for 70/30 (%vol.) NH_3/H_2 under the rich condition of the equivalence ratio 1.1-1.4.

To analyise the origins of these discrepancies between the kinetic mechanisms at rich conditions, Figure 8 shows the sensitivity analysis of the most important reactions that play a considerable role in the laminar flame speed propagation at 1.1, 1.2 and 1.4 of φ. As shown in Figure 8, Gotama, Nakamura and Song kinetic mechanisms present nearly the same elementary reactions that have dominant action in promoting of laminar flame speed such as $H+O_2=O+OH$, $NH_2+NO=NNH+OH$, $OH+H_2=H+H_2O$, and $NH_2+NH=N_2H_2+H$, as well as the reactions with the most substantial influence in retarding the laminar flame speed $H+O_2(+M)=HO_2(+M)$ and $NH_2+H=NH+H_2$. The effect of the mentioned reactions can be seen clearly along the rich conditions. Although the mentioned reactions show a considerable effect on laminar flame speed propagation, their sensitivity coefficient values show different trends due to the variation of Arrhenius parameters among the mechanisms, which in turn govern the reaction rate of each single reaction, table 3.

The difference in estimation of the experimental measurements among the mechanisms can be also justified to the chemistry adopted in each mechanism. According to Figure 8, Gotama kinetic model show the active role of the kinetic reactions $NH_2+NH=N_2H_3$, $NH_2+OH=NH+H_2O$, $NH_2+NH_2=N_2H_3+H$, and $NH_3+OH=NH_2+H_2O$ on the inhibition of laminar flame speed that didn't appear in the other mechanisms. The effect of the mentioned reactions can be seen clearly at 1.1 of φ.

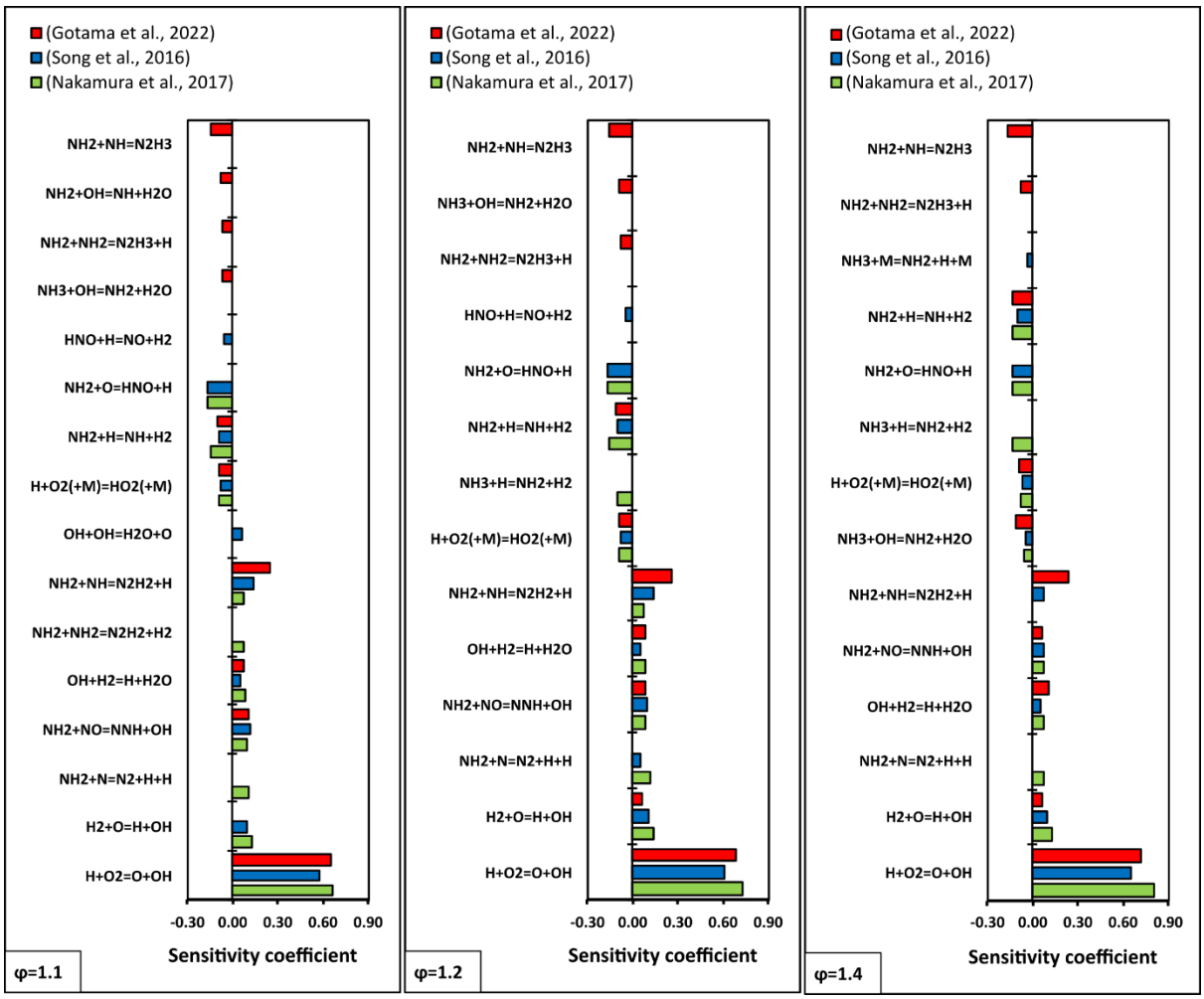

Figure 8: Sensitivity analysis of laminar flame speed for 70/30 (%vol.) NH_3/H_2 under atmospheric conditions and for three kinetic reaction mechanisms (Gotama et al. 2022, Song et al., 2016, and Nakamura et al., 2017) that give a minimum discrepancy value at a rich range of equivalence ratios of 1.1, 1.2, and 1.4.

As can be noticed in Figs. 4 and 7, the reaction models of Gotama, Song, and Nakamura have all overestimated the laminar flame speed under high rich conditions (φ=1.4). However, Nakamura kinetic model is the one that has a better prediction for the experimental data with a low discrepancy value. The sensitivity analysis for Nakamura kinetic model shows that $H+O_2=O+OH$ presents high positive sensitivity values among other important kinetic reactions followed by $H_2+O=H+OH$. Most importantly, the Nakamura mechanism shows the role of both $NH_2+N=N_2+H+H$ and $NH_3+H=NH_2+H_2$ in the promotion and retarding of the flame speed in 70/30 vol% NH_3/H_2, Fig.8. While the absence of the effect of the above-mentioned reactions in the other two mechanisms is apparent, both Gotama and Song's kinetic mechanisms show the importance of $NH_2+NH=N_2H_2+H$ with a sensitivity value between 0.08 and 0.24, Fig. 8.

To investigate the reasons behind the discrepancy among the kinetic mechanisms in estimating the flame speed, Fig. 9 illustrates the reaction rate of the most important kinetic reactions affecting the laminar flame speed for the kinetic mechanisms of Gotama, Song, and Nakamura in terms of temperature and distance for φ =1.4. The figure shows that the reaction rate of the kinetic reaction $H+O_2=O+OH$ estimated by the Gotama mechanism,

has higher value in comparison with the rate of reaction predicted by Song and Nakamura. Along with that, this type of reaction is highly dependent on temperature, as shown in Table 3. Further, as the Gotama mechanism presents a higher reaction rate for $H+O_2=O+OH$ at the reaction zone among other mechanisms, its reaction value decreased sharply when moving away from the reaction zone, this is the case for all reaction mechanisms, and hence goes down underneath Nakamura's reaction rate for the same kinetic reaction. While the kinetic reaction $H+O_2(+M)=HO_2(+M)$ appears in all the selected mechanisms as non-temperature-dependent (because it has zero activation energy), as well as the values of pre-exponential factor (A) and activation energy (E) are nearly the same used for the chosen kinetic models, table 3.

Table 3: Key reactions for the promotion of flame speed of 70/30 VOL% NH_3/H_2 flames at rich conditions and for 3 kinetic mechanisms.

NO.	Reaction	Gotama et al. (2022)			Song et al. (2016)			Nakamura et al. (2017)		
		A	n	E	A	n	E	A	n	E
1	H+O2=O+OH	5.07E+15	-0.5	16126.7	1.00E+14	0	15286	1.04E+14	0	15286
2	NH2+NO=NNH+OH	1.43E+07	1.4	- 1777	3.1E+13	-0.48	1180	3.1E+13	-0.48	1180
3	NH2+H=NH+H2	2.1E+13	0	15417	7.2E+05	2.32	799	6.92E+13	0	3650
4	H+O2(+M) =HO2(+M)	4.65E+12	0.4	0	4.70E+12	0.4	0	4.65E+12	0.4	0

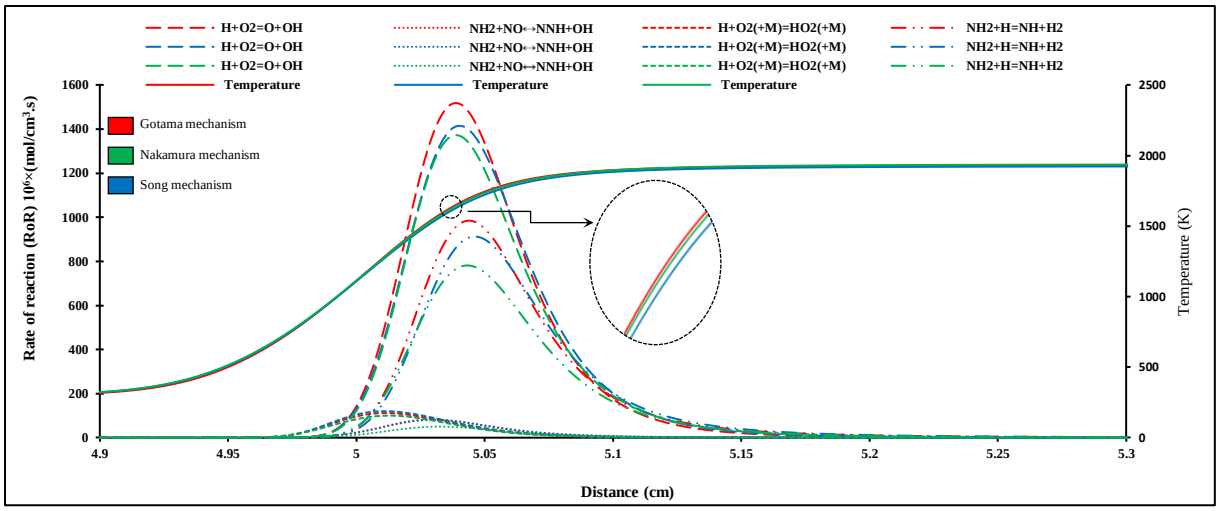

Fig. 9. The rate of reaction profiles of the key reactions for the laminar flame speed of 70/30 (%vol.) NH_3/H_2 flames at φ = 1.4; sold lines refer to the temperature, while dashed lines refer to the rate of reaction.

Finally, Figs. 10 and 11 show the overall performance of the 36 kinetic reaction mechanisms in terms of laminar flame speed estimation from simulations and prediction error based on experimental measurements of the present study, respectively. Fig.10 shows that all the tested mechanisms gave the same distribution pattern of laminar flame speed for various equivalence ratio. The deviation in their estimation for laminar flame speed can be justified for many reasons involving chemistry differentiation and the difference in modelling parameters such as Arrhenius parameters in the estimation of rate of reaction in each single elementary reaction. Fig. 11 indicates the improvement of the prediction of the kinetic reaction when the mixture takes place in the rich conditions with an error between 15% to 13%. Meanwhile, the flame speed prediction accuracy for the kinetic mechanisms deteriorates at the lean range of the equivalence ratio and reaches a high value of under/overestimation close to 38% at 0.6 (φ).

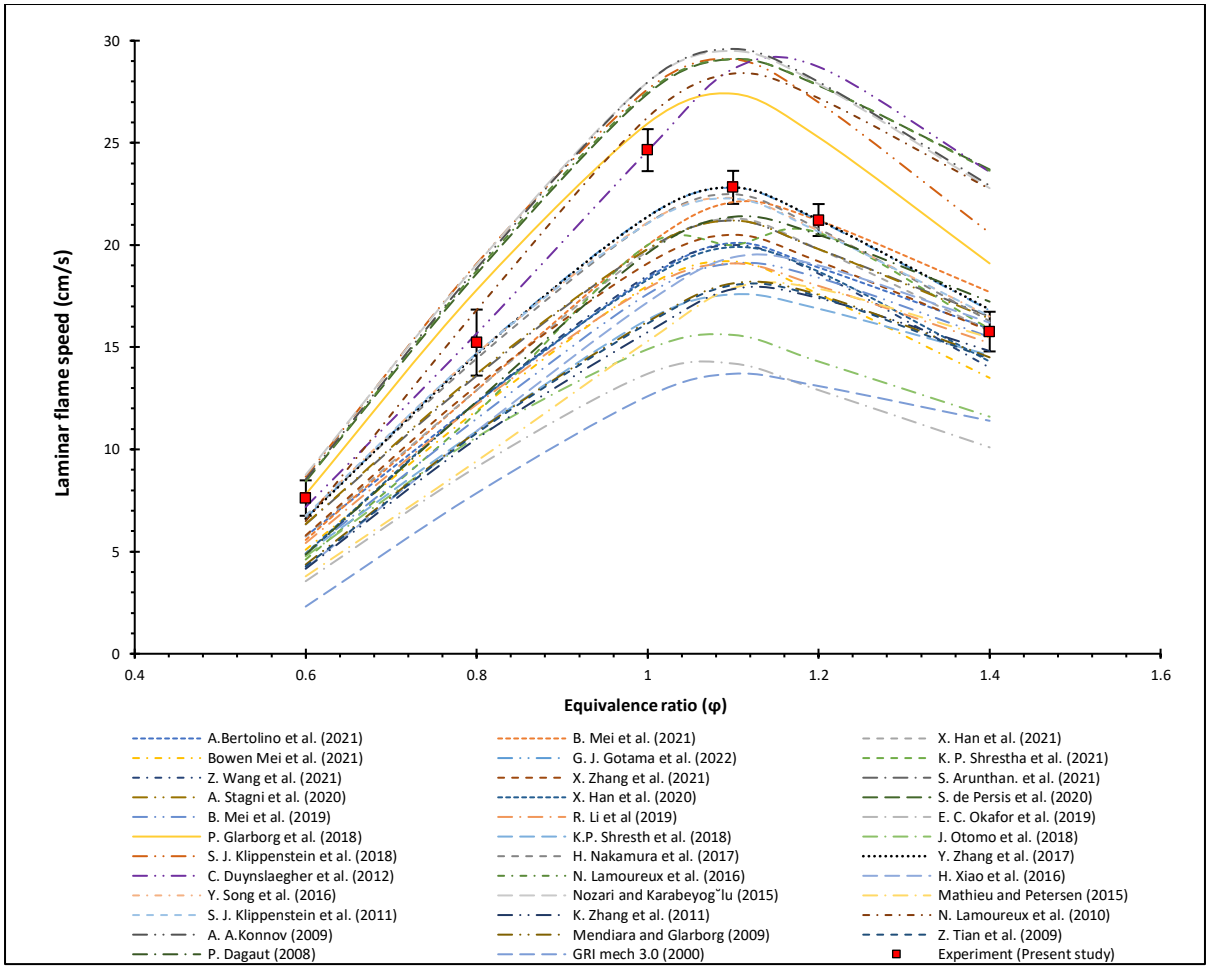

Fig.10. The overall performance of 36 kinetic reaction mechanism for laminar flame speed in terms of various equivalence ratios (0.6-1.4). Dashed lines refers to numerical data, while symbols stand for experimental measurements.

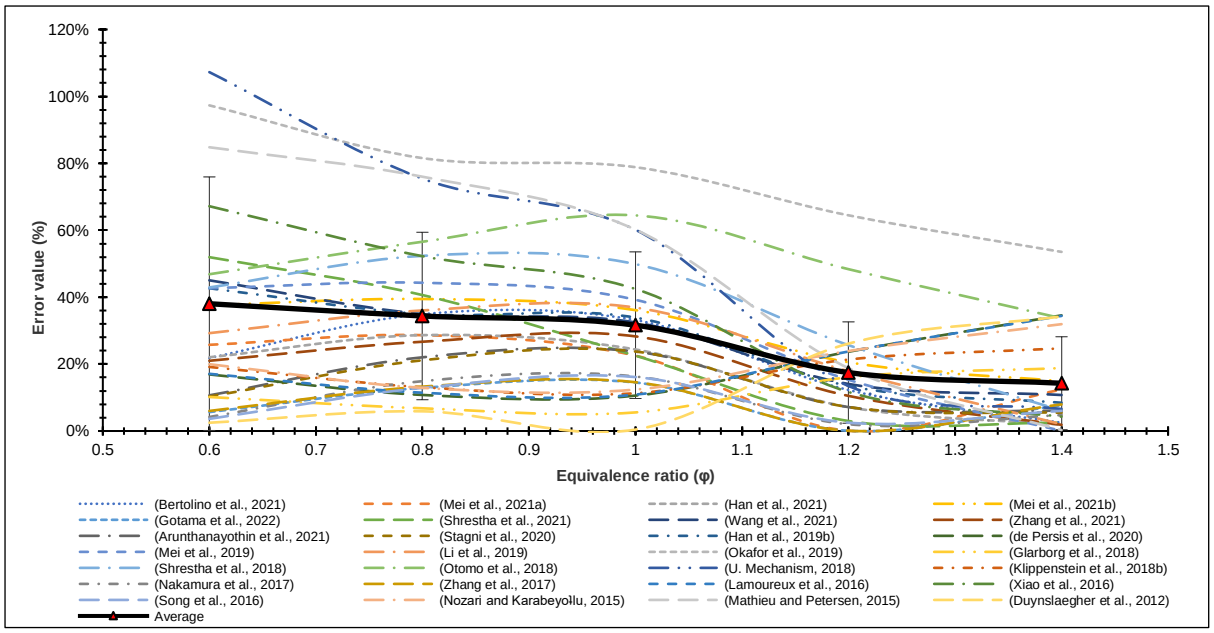

Fig. 11. The trend line of prediction error related to the experimental data on the laminar flame speed of 70/30 (%vol) NH_3/ H_2 blend estimated by kinetic mechanisms investigated as a function of the equivalence ratio; Symbols denote the average prediction error for 36 kinetic model.

Conclusion

The present work investigates the laminar flame speed of 70/30 (%vol.) NH_3/H_2 blended flames for a broad range of the equivalence ratios (0.6-1.4), at atmospheric conditions of pressure and temperature. 36 chemical kinetic mechanisms from the literature were evaluated for their ability to predict Laminar flame speed based on experimental data measured in the present work and previously reported measurements from the literature. The main conclusions are listed as follows:

1. The mechanism of Duynslager provides a very good prediction of the experimental measurements in the lean and stoichiometry conditions of the equivalence ratio (0.6-1.0) with only low levels of a discrepancy between 0% to 6% were observed. While at rich conditions of φ (1.1-1.4), Nakamura kinetic model show better performance in the estimation of laminar flame speed with absolute error range 2% to 8% among other tested mechanisms.
2. The sensitivity analysis shows that each mechanism of the selected mechanisms with better performance in the prediction of laminar flame speed has a different chemistry and demonstrates a reaction routs which aren't shown in other compared mechanisms, such as the kinetic reactions $N_2H_2+M=NNH+H+M$, $NO+O=NO_2$, and $NH_2+H=NH+H_2$' in the promoting/retarding the laminar flame speed at lean conditions described by Duynslaegher kinetic mechanism.
3. The estimation accuracy for the 36 kinetic mechanisms varies along with the equivalence ratio. The majority of kinetic mechanisms over or underestimate the laminar flame speed in the lean conditions, especially at 0.6 of equivalence ratio, where the error bars fluctuate close to 38% of the experimental flame speed. However, the performance of these mechanisms improves at rich conditions with a percentage error close to 13% at 1.4 of φ.

Acknowledgment

The authors gratefully acknowledge the support from EPSRC through the projects SAFE-AGT Pilot (no. EP/T009314/1) and Green Ammonia Thermal Propulsion MariNH3 (no. EP/W016656/1) as well as funding from the European Union's Horizon 2020 research and innovation programme under grant agreement No 884157. Furthermore, Ali Alnasif thanks Al-Furat Al-Awsat Technical University (ATU) for the financial support of his PhD studies in the U.K. Information on the data underpinning the results presented here, including how to access them, can be found in the Cardiff University data catalogue at http://orca.cf.ac.uk/XXXXXX.

References

[1] H. Ritchie, M. Roser, Our World in Data, Available: Https://Ourworldindata.Org/Energy-Production-and-Changing-Energy-Sources. (2020).

[2] A. Riaz, G. Zahedi, J.J. Klemeš, A review of cleaner production methods for the manufacture of methanol, J Clean Prod. 57 (2013) 19–37. https://doi.org/10.1016/j.jclepro.2013.06.017.

[3] W.S. Chai, Y. Bao, P. Jin, G. Tang, L. Zhou, A review on ammonia, ammonia-hydrogen and ammonia-methane fuels, Renewable and Sustainable Energy Reviews. 147 (2021). https://doi.org/10.1016/j.rser.2021.111254.

[4] A. Valera-Medina, H. Xiao, M. Owen-Jones, W.I.F. David, P.J. Bowen, Ammonia for power, Prog Energy Combust Sci. 69 (2018) 63–102. https://doi.org/10.1016/j.pecs.2018.07.001.

[5] A. Valera-Medina, F. Amer-Hatem, A.K. Azad, I.C. Dedoussi, M. De Joannon, R.X. Fernandes, P. Glarborg, H. Hashemi, X. He, S. Mashruk, J. McGowan, C. Mounaim-Rouselle, A. Ortiz-Prado, A. Ortiz-Valera, I. Rossetti, B. Shu, M. Yehia, H. Xiao, M. Costa, Review on ammonia as a potential fuel: From synthesis to economics, Energy and Fuels. 35 (2021) 6964–7029. https://doi.org/10.1021/acs.energyfuels.0c03685.

[6] S. Chatterjee, R.K. Parsapur, K.W. Huang, Limitations of Ammonia as a Hydrogen Energy Carrier for the Transportation Sector, ACS Energy Lett. 6 (2021) 4390–4394. https://doi.org/10.1021/acsenergylett.1c02189.

[7] D.H. Um, T.Y. Kim, O.C. Kwon, Power and hydrogen production from ammonia in a micro-thermophotovoltaic device integrated with a micro-reformer, Energy. 73 (2014) 531–542. https://doi.org/10.1016/j.energy.2014.06.053.

[8] C. Lhuillier, P. Brequigny, F. Contino, C. Mounaïm-Rousselle, Experimental investigation on ammonia combustion behavior in a spark-ignition engine by means of laminar and turbulent expanding flames, in: Proceedings of the Combustion Institute, Elsevier Ltd, 2021: pp. 6671–6678. https://doi.org/10.1016/j.proci.2020.08.058.

[9] C. Lhuillier, P. Brequigny, N. Lamoureux, F. Contino, C. Mounaïm-Rousselle, Experimental investigation on laminar burning velocities of ammonia/hydrogen/air mixtures at elevated temperatures, Fuel. 263 (2020). https://doi.org/10.1016/j.fuel.2019.116653.

[10] C.K. Law, Combustion physics, Cambridge University Press, 2006.

[11] E. Hu, X. Li, X. Meng, Y. Chen, Y. Cheng, Y. Xie, Z. Huang, Laminar flame speeds and ignition delay times of methane-air mixtures at elevated temperatures and pressures, Fuel. 158 (2015) 1–10. https://doi.org/10.1016/j.fuel.2015.05.010.

[12] P.F. Henshaw, T. D'Andrea, K.R.C. Mann, D.S.K. Ting, Premixed ammonia-methane-air combustion, Combustion Science and Technology. 177 (2005) 2151–2170. https://doi.org/10.1080/00102200500240695.

[13] U.J. Pfahl, M.C. Ross, J.E. Shepherd, K.O. Pasamehmetoglu, C. Unal, Flammability Limits, Ignition Energy, and Flame Speeds in H 2-CH 4-NH 3-N 2 O-O 2-N 2 Mixtures, 2000.

[14] J.H. Lee, S.I. Lee, O.C. Kwon, Effects of ammonia substitution on hydrogen/air flame propagation and emissions, Int J Hydrogen Energy. 35 (2010) 11332–11341. https://doi.org/10.1016/j.ijhydene.2010.07.104.

[15] J. Li, H. Huang, N. Kobayashi, Z. He, Y. Osaka, T. Zeng, Numerical study on effect of oxygen content in combustion air on ammonia combustion, Energy. 93 (2015) 2053–2068. https://doi.org/10.1016/j.energy.2015.10.060.

[16] H. TAKEISHI, J. HAYASHI, S. KONO, W. ARITA, K. IINO, F. AKAMATSU, Characteristics of ammonia/N_2/O_2 laminar flame in oxygen-enriched air condition, Transactions of the JSME (in Japanese). 81 (2015) 14-00423-14–00423. https://doi.org/10.1299/transjsme.14-00423.

[17] C.S. Mørch, A. Bjerre, M.P. Gøttrup, S.C. Sorenson, J. Schramm, Ammonia/hydrogen mixtures in an SI-engine: Engine performance and analysis of a proposed fuel system, Fuel. 90 (2011) 854–864. https://doi.org/10.1016/j.fuel.2010.09.042.

[18] A. Ichikawa, A. Hayakawa, Y. Kitagawa, K.D. Kunkuma Amila Somarathne, T. Kudo, H. Kobayashi, Laminar burning velocity and Markstein length of ammonia/hydrogen/air premixed flames at elevated pressures, Int J Hydrogen Energy. 40 (2015) 9570–9578. https://doi.org/10.1016/j.ijhydene.2015.04.024.

[19] J. Chen, X. Jiang, X. Qin, Z. Huang, Effect of hydrogen blending on the high temperature auto-ignition of ammonia at elevated pressure, Fuel. 287 (2021). https://doi.org/10.1016/j.fuel.2020.119563.

[20] J. Li, H. Huang, N. Kobayashi, C. Wang, H. Yuan, Numerical study on laminar burning velocity and ignition delay time of ammonia flame with hydrogen addition, Energy. 126 (2017) 796–809. https://doi.org/10.1016/j.energy.2017.03.085.

[21] B. Mei, J. Zhang, X. Shi, Z. Xi, Y. Li, Enhancement of ammonia combustion with partial fuel cracking strategy: Laminar flame propagation and kinetic modeling investigation of NH3/H2/N2/air mixtures up to 10 atm, Combust Flame. 231 (2021). https://doi.org/10.1016/j.combustflame.2021.111472.

[22] P. Glarborg, J.A. Miller, B. Ruscic, S.J. Klippenstein, Modeling nitrogen chemistry in combustion, Prog Energy Combust Sci. 67 (2018) 31–68. https://doi.org/10.1016/j.pecs.2018.01.002.

[23] S.J. Klippenstein, M. Pfeifle, A.W. Jasper, P. Glarborg, Theory and modeling of relevance to prompt-NO formation at high pressure, Combust Flame. 195 (2018) 3–17. https://doi.org/10.1016/j.combustflame.2018.04.029.

[24] K.P. Shrestha, C. Lhuillier, A.A. Barbosa, P. Brequigny, F. Contino, C. Mounaïm-Rousselle, L. Seidel, F. Mauss, An experimental and modeling study of ammonia with enriched oxygen content and ammonia/hydrogen laminar flame speed at elevated pressure and temperature, Proceedings of the Combustion Institute. 38 (2021) 2163–2174. https://doi.org/10.1016/j.proci.2020.06.197.

[25] K.P. Shrestha, L. Seidel, T. Zeuch, F. Mauss, Detailed Kinetic Mechanism for the Oxidation of Ammonia Including the Formation and Reduction of Nitrogen Oxides, Energy and Fuels. 32 (2018) 10202–10217. https://doi.org/10.1021/acs.energyfuels.8b01056.

[26] O. Mathieu, E.L. Petersen, Experimental and modeling study on the high-temperature oxidation of Ammonia and related NOx chemistry, Combust Flame. 162 (2015) 554–570. https://doi.org/10.1016/j.combustflame.2014.08.022.

[27] R. Li, A.A. Konnov, G. He, F. Qin, D. Zhang, Chemical mechanism development and reduction for combustion of NH3/H2/CH4 mixtures, Fuel. 257 (2019). https://doi.org/10.1016/j.fuel.2019.116059.

[28] B. Galmiche, F. Halter, F. Foucher, Effects of high pressure, high temperature and dilution on laminar burning velocities and Markstein lengths of iso-octane/air mixtures, Combust Flame. 159 (2012) 3286–3299. https://doi.org/10.1016/j.combustflame.2012.06.008.

[29] S. Zitouni, D. Pugh, A. Crayford, P.J. Bowen, J. Runyon, Lewis number effects on lean premixed combustion characteristics of multi-component fuel blends, Combust Flame. 238 (2022). https://doi.org/10.1016/j.combustflame.2021.111932.

[30] A.P. Kelley, C.K. Law, Nonlinear effects in the extraction of laminar flame speeds from expanding spherical flames, Combust Flame. 156 (2009) 1844–1851. https://doi.org/10.1016/j.combustflame.2009.04.004.

[31] Z. Chen, On the accuracy of laminar flame speeds measured from outwardly propagating spherical flames: Methane/air at normal temperature and pressure, Combust Flame. 162 (2015) 2442–2453. https://doi.org/10.1016/j.combustflame.2015.02.012.

[32] R.J. Moffat, Describing the uncertainties in experimental results, Exp Therm Fluid Sci. 1 (1988) 3–17. https://doi.org/10.1016/0894-1777(88)90043-X.

[33] P. Brequigny, H. Uesaka, Z. Sliti, D. Segawa, F. Foucher, G. Dayma, C. Mounaïm-Rousselle, Uncertainty in measuring laminar burning velocity from expanding methane-air flames at low pressures, n.d. https://hal.archives-ouvertes.fr/hal-02163518.

[34] F. Wu, W. Liang, Z. Chen, Y. Ju, C.K. Law, Uncertainty in stretch extrapolation of laminar flame speed from expanding spherical flames, Proceedings of the Combustion Institute. 35 (2015) 663–670. https://doi.org/10.1016/j.proci.2014.05.065.

[35] A. Bertolino, M. Fürst, A. Stagni, A. Frassoldati, M. Pelucchi, C. Cavallotti, T. Faravelli, A. Parente, An evolutionary, data-driven approach for mechanism optimization: theory and application to ammonia combustion, Combust Flame. 229 (2021). https://doi.org/10.1016/j.combustflame.2021.02.012.

[36] F.A. William, S. Kalyanasundaram, R.J. Cattolica, San Diego Mech, Chemical-Kinetic Mechanisms for Combustion Applications, San Diego Mech. Web Page, Mech. Aerosp. Eng. Combustion Res. Univ. Calif. San Diego. (2012).

[37] B. Mei, S. Ma, X. Zhang, Y. Li, Characterizing ammonia and nitric oxide interaction with outwardly propagating spherical flame method, Proceedings of the Combustion Institute. 38 (2021) 2477–2485. https://doi.org/10.1016/j.proci.2020.07.133.

[38] X. Han, L. Lavadera, A.A. Konnov, An experimental and kinetic modeling study on the laminar burning velocity of NH3+N2O+air flames, Combust Flame. 228 (2021) 13–28. https://doi.org/10.1016/j.combustflame.2021.01.027.

[39] H. Nakamura, S. Hasegawa, T. Tezuka, Kinetic modeling of ammonia/air weak flames in a micro flow reactor with a controlled temperature profile, Combust Flame. 185 (2017) 16–27. https://doi.org/10.1016/j.combustflame.2017.06.021.

[40] Y. Zhang, O. Mathieu, E.L. Petersen, G. Bourque, H.J. Curran, Assessing the predictions of a NOx kinetic mechanism on recent hydrogen and syngas experimental data, Combust Flame. 182 (2017) 122–141. https://doi.org/10.1016/j.combustflame.2017.03.019.

[41] G.J. Gotama, A. Hayakawa, E.C. Okafor, R. Kanoshima, M. Hayashi, T. Kudo, H. Kobayashi, Measurement of the laminar burning velocity and kinetics study of the importance of the hydrogen recovery mechanism of ammonia/hydrogen/air premixed flames, Combust Flame. 236 (2022). https://doi.org/10.1016/j.combustflame.2021.111753.

[42] N. Lamoureux, H. El Merhubi, L. Pillier, S. de Persis, P. Desgroux, Modeling of NO formation in low pressure premixed flames, Combust Flame. 163 (2016) 557–575. https://doi.org/10.1016/j.combustflame.2015.11.007.

[43] H. Xiao, A. Valera-Medina, Chemical Kinetic Mechanism Study on Premixed Combustion of Ammonia/Hydrogen Fuels for Gas Turbine Use, J Eng Gas Turbine Power. 139 (2017). https://doi.org/10.1115/1.4035911.

[44] Z. Wang, X. Han, Y. He, R. Zhu, Y. Zhu, Z. Zhou, K. Cen, Experimental and kinetic study on the laminar burning velocities of NH3 mixing with CH3OH and C2H5OH in premixed flames, Combust Flame. 229 (2021). https://doi.org/10.1016/j.combustflame.2021.02.038.

[45] Y. Song, H. Hashemi, J.M. Christensen, C. Zou, P. Marshall, P. Glarborg, Ammonia oxidation at high pressure and intermediate temperatures, Fuel. 181 (2016) 358–365. https://doi.org/10.1016/j.fuel.2016.04.100.

[46] X. Zhang, S.P. Moosakutty, R.P. Rajan, M. Younes, S.M. Sarathy, Combustion chemistry of ammonia/hydrogen mixtures: Jet-stirred reactor measurements and comprehensive kinetic modeling, Combust Flame. 234 (2021). https://doi.org/10.1016/j.combustflame.2021.111653.

[47] H. Nozari, A. Karabeyoğlu, Numerical study of combustion characteristics of ammonia as a renewable fuel and establishment of reduced reaction mechanisms, Fuel. 159 (2015) 223–233. https://doi.org/10.1016/j.fuel.2015.06.075.

[48] S. Arunthanayothin, A. Stagni, Y. Song, O. Herbinet, T. Faravelli, F. Battin-Leclerc, Ammonia-methane interaction in jet-stirred and flow reactors: An experimental and kinetic modeling study, in: Proceedings of the Combustion Institute, Elsevier Ltd, 2021: pp. 345–353. https://doi.org/10.1016/j.proci.2020.07.061.

[49] A. Stagni, C. Cavallotti, S. Arunthanayothin, Y. Song, O. Herbinet, F. Battin-Leclerc, T. Faravelli, An experimental, theoretical and kinetic-modeling study of the gas-phase oxidation of ammonia, React Chem Eng. 5 (2020) 696–711. https://doi.org/10.1039/c9re00429g.

[50] C. Duynslaegher, F. Contino, J. Vandooren, H. Jeanmart, Modeling of ammonia combustion at low pressure, Combust Flame. 159 (2012) 2799–2805. https://doi.org/10.1016/j.combustflame.2012.06.003.

[51] X. Han, Z. Wang, M. Costa, Z. Sun, Y. He, K. Cen, Experimental and kinetic modeling study of laminar burning velocities of NH3/air, NH3/H2/air, NH3/CO/air and NH3/CH4/air premixed flames, Combust Flame. 206 (2019) 214–226. https://doi.org/10.1016/j.combustflame.2019.05.003.

[52] S.J. Klippenstein, L.B. Harding, P. Glarborg, J.A. Miller, The role of NNH in NO formation and control, Combust Flame. 158 (2011) 774–789. https://doi.org/10.1016/j.combustflame.2010.12.013.

[53] S. de Persis, L. Pillier, M. Idir, J. Molet, N. Lamoureux, P. Desgroux, NO formation in high pressure premixed flames: Experimental results and validation of a new revised reaction mechanism, Fuel. 260 (2020). https://doi.org/10.1016/j.fuel.2019.116331.

[54] K. Zhang, Y. Li, T. Yuan, J. Cai, P. Glarborg, F. Qi, An experimental and kinetic modeling study of premixed nitromethane flames at low pressure, Proceedings of the Combustion Institute. 33 (2011) 407–414. https://doi.org/10.1016/j.proci.2010.06.002.

[55] B. Mei, X. Zhang, S. Ma, M. Cui, H. Guo, Z. Cao, Y. Li, Experimental and kinetic modeling investigation on the laminar flame propagation of ammonia under oxygen enrichment and elevated pressure conditions, Combust Flame. 210 (2019) 236–246. https://doi.org/10.1016/j.combustflame.2019.08.033.

[56] N. Lamoureux, P. Desgroux, A. El Bakali, J.F. Pauwels, Experimental and numerical study of the role of NCN in prompt-NO formation in low-pressure CH4-O2-N2 and C2H2-O2-N2 flames, Combust Flame. 157 (2010) 1929–1941. https://doi.org/10.1016/j.combustflame.2010.03.013.

[57] A.A. Konnov, Implementation of the NCN pathway of prompt-NO formation in the detailed reaction mechanism, Combust Flame. 156 (2009) 2093–2105. https://doi.org/10.1016/j.combustflame.2009.03.016.

[58] E.C. Okafor, Y. Naito, S. Colson, A. Ichikawa, T. Kudo, A. Hayakawa, H. Kobayashi, Experimental and numerical study of the laminar burning velocity of CH4–NH3–air premixed flames, Combust Flame. 187 (2018) 185–198. https://doi.org/10.1016/J.COMBUSTFLAME.2017.09.002.

[59] T. Mendiara, P. Glarborg, Ammonia chemistry in oxy-fuel combustion of methane, Combust Flame. 156 (2009) 1937–1949. https://doi.org/10.1016/j.combustflame.2009.07.006.

[60] Z. Tian, Y. Li, L. Zhang, P. Glarborg, F. Qi, An experimental and kinetic modeling study of premixed NH3/CH4/O2/Ar flames at low pressure, Combust Flame. 156 (2009) 1413–1426. https://doi.org/10.1016/j.combustflame.2009.03.005.

[61] P. Dagaut, P. Glarborg, M.U. Alzueta, The oxidation of hydrogen cyanide and related chemistry, Prog Energy Combust Sci. 34 (2008) 1–46. https://doi.org/10.1016/j.pecs.2007.02.004.

[62] J. Otomo, M. Koshi, T. Mitsumori, H. Iwasaki, K. Yamada, Chemical kinetic modeling of ammonia oxidation with improved reaction mechanism for ammonia/air and ammonia/hydrogen/air combustion, Int J Hydrogen Energy. 43 (2018) 3004–3014. https://doi.org/10.1016/j.ijhydene.2017.12.066.

[63] Gregory P. Smith, David M. Golden, Michael Frenklach, Nigel W. Moriarty, Boris Eiteneer, Mikhail Goldenberg, C. Thomas Bowman, Ronald K. Hanson, Soonho Song, William C. Gardiner, V.V.L. Jr., Zhiwei Qin, GRI-Mech 3.0, Http://Www.Me.Berkeley.Edu/Gri_mech/. (2000).

[64] J.S. Armstrong, F. Collopy, Error measures for generalizing about forecasting methods: Empirical comparisons *, 1992.

[65] Z. Chen, On the extraction of laminar flame speed and Markstein length from outwardly propagating spherical flames, Combust Flame. 158 (2011) 291–300. https://doi.org/10.1016/J.COMBUSTFLAME.2010.09.001.